

Mechanism for Enhanced Disordered Screening in Strongly Correlated Metals: Local vs. Nonlocal Effects

Eric C. Andrade · Eduardo Miranda ·
Vladimir Dobrosavljević

Received: 18 May 2012 / Accepted: 20 May 2012 / Published online: 6 June 2012
© Springer Science+Business Media, LLC 2012

Abstract We study the low temperature transport characteristics of a disordered metal in the presence of electron–electron interactions. We compare Hartree–Fock and dynamical mean field theory (DMFT) calculations to investigate the scattering processes of quasiparticles off the screened disorder potential and show that both the local and non-local (coming from long-ranged Friedel oscillations) contributions to the renormalized disorder potential are suppressed in strongly renormalized Fermi liquids. Our results provide one more example of the power of DMFT to include higher order terms left out by weak-coupling theories.

Keywords Disorder · Strong correlations · Perturbation theory · Dynamical mean-field theory

1 Introduction

Transport in dirty metals has been investigated for many years, with a substantial theoretical and experimental un-

derstanding being achieved in the case of weak disorder and moderate electron–electron interaction [1, 2]. However, much less is known about situations with strong electronic correlations, where much of our understanding relies on the application of numerical methods like quantum Monte Carlo [3] or exact diagonalization [4], which are nevertheless severely limited in temperature range and system sizes. A more flexible approach to investigate the interplay of strong correlations and disorder is provided by the dynamical mean field theory (DMFT) [5]. In its original formulation, the DMFT treatment of disordered systems does not include Anderson localization effects [6], a limitation which was quickly resolved by the introduction of the statistical DMFT (statDMFT) [7, 8]. The statDMFT approach has already led to some novel effects like a strong disorder screening by interactions [6, 9], energy-resolved spatial inhomogeneities [9], and the emergence of an Electronic Griffiths phase in the vicinity of the disordered Mott transition [10, 11].

To partially elucidate the mechanism behind the rich physics uncovered through the statDMFT method, a recent work [12] provided analytical insights into the scattering off a weak random disorder potential in an otherwise uniform strongly interacting paramagnetic metal. While the analysis is most straightforward and transparent in this regime, this general issue is of key relevance also for the diffusive regime. Here, we revisit this problem, explicitly comparing the statDMFT results with those of the Hartree–Fock (HF) approximation. Our analytical results highlight the non-perturbative nature of the statDMFT and show that processes left out by HF generate vertex corrections to the impurity potential, which ultimately lead to enhanced screening [6].

E.C. Andrade
Institut für Theoretische Physik, Technische Universität Dresden,
01062 Dresden, Germany

E. Miranda
Instituto de Física Gleb Wataghin, Unicamp, Campinas,
SP 13083-859, Brazil

V. Dobrosavljević (✉)
Department of Physics and National High Magnetic Field
Laboratory, Florida State University, Tallahassee, FL 32306, USA
e-mail: vlad@magnet.fsu.edu

2 Model and Methods

We study the paramagnetic phase of the disordered Hubbard model

$$\mathcal{H} = \sum_{i\sigma} \varepsilon_i n_{i\sigma} - \sum_{\langle ij \rangle, \sigma} t_{ij} c_{i\sigma}^\dagger c_{j\sigma} + U \sum_i n_{i\uparrow} n_{i\downarrow}, \quad (1)$$

where t_{ij} are the hopping matrix elements between nearest-neighbor sites, $c_{i\sigma}^\dagger$ ($c_{i\sigma}$) is the creation (annihilation) operator of an electron with spin projection σ at site i , U is the on-site Hubbard repulsion, $n_{i\sigma} = c_{i\sigma}^\dagger c_{i\sigma}$ is the number operator, and ε_i are the site energies (bare disorder potential). We consider here its paramagnetic phase at half-filling (chemical potential $\mu = U/2$) and a particle-hole symmetric lattice. Below we discuss two different routes to treat this model.

2.1 Hartree–Fock (HF)

To solve model (Eq. 1), we first consider the HF approach, as described, for example, in [13, 14]. Here, we simply decouple the interaction term in Eq. 1 as $n_{i\uparrow} n_{i\downarrow} \approx \langle n_{i\uparrow} \rangle n_{i\downarrow} + n_{i\uparrow} \langle n_{i\downarrow} \rangle - \langle n_{i\uparrow} \rangle \langle n_{i\downarrow} \rangle$. We restrict ourselves to the paramagnetic solution, $\langle n_{i\uparrow} \rangle = \langle n_{i\downarrow} \rangle = \langle n_i \rangle$, and the self-consistency condition is obtained from

$$\langle n_i \rangle = T \sum_{\omega_n} G_{ii}(\omega_n) = T \sum_{\omega_n} \left[\frac{1}{i\omega_n \mathbf{1} - \mathbf{v} - \mathcal{H}_0} \right]_{ii}, \quad (2)$$

where T is the temperature, $G_{ii}(\omega_n)$ is the local part of the lattice Green's function, ω_n are the Matsubara frequencies, \mathcal{H}_0 is the clean ($\varepsilon_i = 0$) and non-interacting ($U = 0$) lattice Hamiltonian, \mathbf{v} is a site-diagonal matrix [\mathbf{v}] $_{ij} = v_i \delta_{ij}$, whose entries

$$v_i = \varepsilon_i + \Sigma_i(0) - \mu = \varepsilon_i + U \langle n_i \rangle - \mu \quad (3)$$

are the renormalized HF disorder potential, and $\Sigma_i(0) = \Sigma_i(\omega) = U \langle n_i \rangle$ is the frequency-independent HF electronic self-energy. We note that the HF approximation can be regarded as the static (weak-coupling) limit of the statDMFT and that it already contains one of its most important features: a self-energy which is local, but which varies from site to site reflecting spatial disorder fluctuations. As we will show later, the statDMFT contains all the HF diagrams, but it also re-sums many higher order terms left out by HF.

In general, we have to solve the self-consistency equation in Eq. 2 numerically. However, for a weak disorder potential ($|\varepsilon_i| \ll D$, where D is the bare half bandwidth), we can expand it around the uniform solution, and, to leading order in the disorder potential, we have

$$v(\mathbf{q}) = \frac{\varepsilon(\mathbf{q})}{1 - U\Pi_{\mathbf{q}}} + \mathcal{O}[\varepsilon(\mathbf{q})^2], \quad (4)$$

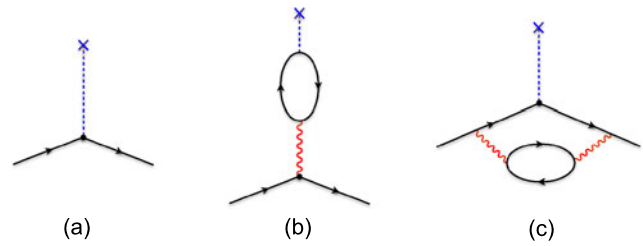


Fig. 1 Diagrammatic representation of the electron–impurity interaction: (a) the bare electron–impurity interaction vertex; (b) the first term of the Hartree–Fock theory, which is equivalent to the RPA re-summation of “bubbles”; (c) the first vertex correction to the electron–impurity interaction, absent in Hartree–Fock theory, but included in the statDMFT/slave boson solution. The inclusion of these and higher-order vertex corrections is essential for the phenomenon of perfect disorder screening. Here, the wavy line corresponds to the local on-site Hubbard-type electron–electron interaction

where $\varepsilon(\mathbf{q})$ is the inverse lattice Fourier transform of the disorder potential ε_i . $\Pi_{\mathbf{q}}$ is the usual static Lindhard polarization function [15].

As $U \rightarrow 0$, the renormalized disorder potential reads $v_i \simeq \varepsilon_i + U\Pi_{ij}\varepsilon_j$, where Π_{ij} is the lattice Fourier transform of $\Pi_{\mathbf{q}}$, showing that the electrons scatter not only off the bare impurities, but also off the long-ranged potential generated by the Friedel oscillations (encoded in Π_{ij}). This result contains another general feature of the statDMFT: the renormalized disorder potential acquires non-local terms, which are absent in the original DMFT formulation [6].

We can easily interpret Eq. 4 in terms of the usual diagrammatic perturbation theory if we rewrite it as

$$\frac{v(\mathbf{q})}{\varepsilon(\mathbf{q})} = \frac{1}{\kappa_{\text{RPA}}(\mathbf{q})} = 1 + U_{\text{eff}}^{\text{HF}}(\mathbf{q})\Pi_{\mathbf{q}}, \quad (5)$$

$$U_{\text{eff}}^{\text{HF}}(\mathbf{q}) = \frac{U}{1 - U\Pi_{\mathbf{q}}} = \frac{U}{\kappa_{\text{RPA}}(\mathbf{q})}, \quad (6)$$

where we have defined the dielectric function

$$\kappa_{\text{RPA}}(\mathbf{q}) = 1 - U\Pi_{\mathbf{q}}, \quad (7)$$

which in this approximation is given by the RPA expression [15]. It is then clear that the HF approximation dresses the electron–impurity vertex by a “chain of bubbles”, as in the standard RPA screening theory [15], Fig. 1b.

2.2 Slave-Bosons (SB)

To investigate the strongly correlated regime, we implement the statDMFT using the slave-boson (SB) mean-field theory of Kotliar and Ruckenstein [16] (which is equivalent to the Gutzwiller variational approximation [17]) as impurity solver [9, 11]. This theory is mathematically equivalent to applying directly the original formulation of Kotliar and Ruckenstein to the Hubbard model in Eq. 1, as discussed in [9].

As in the previous HF calculation, we consider a weak disorder potential and expand the relevant mean-field equations [9, 11] around their uniform solution. For particle–hole symmetry $Z_i = Z_0 + \mathcal{O}(\varepsilon_i^2)$ and we have, at $T = 0$ [12]

$$v(\mathbf{q}) = \frac{\varepsilon(\mathbf{q})}{1 - u^2 - \tilde{U}\Pi_{\mathbf{q}}} + \mathcal{O}[\varepsilon(\mathbf{q})^2], \tag{8}$$

where $u = U/U_c$ and

$$\tilde{U} = \left(\frac{u}{2} - \frac{1}{1-u}\right)U. \tag{9}$$

Equation 8 implies the following dielectric function

$$\kappa_{\text{SB}}(\mathbf{q}) = 1 - u^2 - \tilde{U}\Pi_{\mathbf{q}}. \tag{10}$$

The relation $n(\mathbf{q}) = 1/2 + \Pi_{\mathbf{q}}v(\mathbf{q})$ also holds, as expected. It is instructive to consider the limits of weak and strong interactions. If $U \ll U_c$,

$$\kappa_{\text{SB}}(\mathbf{q}) \approx 1 - U\Pi_{\mathbf{q}} = \kappa_{\text{RPA}}(\mathbf{q}), \tag{11}$$

and we recover the HF result. In contrast, as $U \rightarrow U_c$,

$$\kappa_{\text{SB}}(\mathbf{q}) \rightarrow -\frac{U_c}{1-u}\Pi_{\mathbf{q}}, \tag{12}$$

leading to

$$v_i \simeq -(1 - U/U_c)U_c^{-1}[\Pi^{-1}]_{ij}\varepsilon_j. \tag{13}$$

As the system approaches the Mott transition, the renormalized disorder potential goes to zero at all lattice sites, a situation that was dubbed “perfect disorder screening” in [6]. Its spatial structure is also very interesting, since v_i is just as non-local as for small U , but the non-local term is governed not by the Lindhard function, but by its inverse. The spatial structure of the charge disturbance in this limit is given by

$$\delta n_i = [(1 - U/U_c)/U_c]\varepsilon_i + \mathcal{O}((1 - U/U_c)^3). \tag{14}$$

Thus, although the charge fluctuations are suppressed everywhere, its non-local part, coming from the Friedel oscillations, is much more strongly suppressed ($\mathcal{O}(1 - u)^3$) and the electronic density is significantly disturbed only in the immediate vicinity of the impurities. The suppression of the slow spatial decay in δn_i reflects the fundamental tendency of quasiparticles to become localized as the system approaches the Mott insulator. Therefore, density fluctuations are healed very effectively in the strongly correlated limit.

Additional insight into these results can be obtained by noting that the second term on the right-hand side of Eq. 10 is unimportant both in the weakly and in the strongly correlated limits, cf. Eqs. 11 and 12. Neglecting this term in

Eq. 10, we can follow the same procedure as in Eq. 5 and rewrite Eq. 8 as

$$\frac{v(\mathbf{q})}{\varepsilon(\mathbf{q})} = 1 + U_{\text{eff}}^{\text{SB}}(\mathbf{q})\Pi_{\mathbf{q}}, \tag{15}$$

$$U_{\text{eff}}^{\text{SB}}(\mathbf{q}) = \frac{\tilde{U}}{1 - \tilde{U}\Pi_{\mathbf{q}}}. \tag{16}$$

The approach to Mott localization in this language can thus be described by the replacement $U \rightarrow \tilde{U}$, cf. Eqs. 5 and 6. This replacement, in turn, may be viewed as a *local field correction* coming from vertex corrections in the polarization function [15, 18] (see Fig. 1(c) and the discussion in Sect. 3 below). Close to the Mott transition $\tilde{U} \approx U/(1 - u)$ diverges and this strong correlation effect is seen to fall completely outside the scope of the HF theory. In fact, whereas HF predicts a gradual decrease of the dielectric function with increasing U , signaling the suppressed screening, see Eq. 7, the statDMFT/SB approach predicts precisely the opposite: the dielectric function diverges as $U \rightarrow U_c$, see Eq. 12, and the screening becomes *asymptotically perfect*.

3 Beyond Weak-Coupling

Comparing the renormalized disorder potential in Eqs. 4 and 8, we see that the interaction corrections left out by HF generate vertex corrections to the impurity potential, which are contained in the effective interaction $U_{\text{eff}}^{\text{SB}}(\mathbf{q})$ in Eq. 16. Since the HF approximation is the first term in expanding the electronic self-energy in U , we expand our solutions Eqs. 4 and 8 in powers of U , in order to track down which terms are left out of HF. As we have seen, to first order in U , the statDMFT/SB and HF solutions agree. At second order, a difference emerges already

$$\frac{v_{\text{HF}}^{(2)}(\mathbf{q})}{\varepsilon(\mathbf{q})} = U^2\Pi_{\mathbf{q}}^2, \tag{17}$$

$$\frac{v_{\text{SB}}^{(2)}(\mathbf{q})}{\varepsilon(\mathbf{q})} = U^2\Pi_{\mathbf{q}}^2 + \left(\frac{U}{U_c}\right)^2\left(1 + \frac{3}{2}U_c\Pi_{\mathbf{q}}\right). \tag{18}$$

To gain insight into the leading correction beyond HF, we combine the statDMFT procedure with usual perturbation theory. First, we recall that in the statDMFT approach the electronic self-energy is local, albeit site-dependent. The only contribution to a local self-energy which is of second order in the interactions is given by [19]

$$\Sigma_i^{(2)}(i\omega_n) = U^2T \sum_{v_n} G_{ii}^{(0)}(i\omega_n + iv_n)\Pi_{ii}(iv_n), \tag{19}$$

where

$$\Pi_{ii}(iv_n) = T \sum_{v'_n} G_{ii}^{(0)}(iv'_n)G_{ii}^{(0)}(iv'_n - iv_n) \tag{20}$$

is the local contribution of the dynamical Lindhard polarization, calculated using the local Green's function $G_{ii}^{(0)}(i\omega_n) = [(i\omega_n - \epsilon - \mathcal{H}_0)^{-1}]_{ii}$ with $\epsilon_{ij} = \epsilon_i \delta_{ij}$. We are interested only in the leading ω_n behavior of Eq. 19, since our statDMFT/SB approach is itself a low-energy one [20]. Ultimately, this low-energy approximation provides a local Fermi-liquid description of the auxiliary impurity problem [21]. For example, the uniform contribution ($\epsilon_i = 0$) of Eq. 19 is $\Sigma_0^{(2)}(i\omega_n) \approx (1 - 1/Z_0^{(2)})i\omega_n + \mathcal{O}(\omega_n^2)$, with $(1 - 1/Z_0^{(2)}) \propto -U^2$, for a particle-hole symmetric lattice.

We now expand Eqs. 19 and 20 to linear order in the impurity potential. There are three identical contributions, each with one of the three Green's function lines with an impurity vertex inserted in it, as shown in Fig. 1(c). We focus on $\Sigma_i^{(2)}(0)$ since this defines the renormalized disorder potential. Qualitatively, it is very easy to see how the extra terms in Eq. 18 are generated. Consider, for simplicity, that we estimate $\Pi_{ii}(i\nu_n)$ in Eq. 19 through the clean and static limit $\Pi_{ii}(i\nu_n) \approx \Pi_0(0) = -\rho(0) \approx -U_c^{-1}$. In this case, we simply have $\Sigma_i^{(2)}(0) \approx (U/U_c)^2 U_c \Pi_{ij} \epsilon_j$, which has the same structure as the last term in Eq. 18. Based on these arguments, we stress that the difference which exists already at order U^2 between Eqs. 17 and 18 is an interaction-generated vertex correction of the electron–impurity vertex, which is absent in HF/RPA screening theory, but which is re-summed to all orders within statDMFT/SB.

4 Conclusions

We presented a detailed analytical calculation of the effects of weak disorder scattering in a correlated host. Comparing the results obtained within HF and statDMFT, we highlighted the fact that statDMFT incorporates important vertex corrections to all orders, a task which is difficult, or more likely, even impossible to perform using weak-coupling diagrammatic approaches. A physical consequence of the inclusion of these vertex corrections is the phenomenon of disorder screening by interactions.

An analogous example of this dichotomy can be observed in the familiar Migdal–Eliashberg (ME) strong coupling theory describing the electron–phonon problem [15]. Indeed, the ME theory neglects the momentum dependence of the electronic self-energy and may thus be regarded as a weak-coupling approximation to DMFT. Like the HF/RPA screening described above, it also neglects vertex corrections. The full DMFT solution, however, not only contains all the ME diagrams, but it also re-sums many higher order terms left out by the ME approach, including vertex corrections [22], in close analogy with the statDMFT treatment of disorder

and interactions. In both models, these strong coupling effects reflect non-perturbative Kondo-like processes [6, 22], which cannot be described by weak-coupling approaches.

In the future, it will be interesting to study the behavior of a finite concentration of impurities, considering for instance non-trivial impurity configurations (e.g., stripes [23]). In the context of high temperature cuprate superconductors, a non-trivial self-organization of dopants was recently observed to be associated with the onset of high-quality superconductivity [24, 25], pointing once more to the significant effects of spatial inhomogeneities in strongly correlated phases [26].

Acknowledgements This research was supported by the DFG through FOR 960 and GRK 1621 (ECA), by FAPESP through grant 07/57630-5 (EM), CNPq through grant 304311/2010-3 (EM), and by the NSF through grant DMR-0542026 (VD). The authors thank Lev Gor'kov for pointing out the role of vertex corrections in the Holstein model.

References

1. Lee, P.A., Ramakrishnan, T.V.: *Rev. Mod. Phys.* **57**, 287 (1985)
2. Punnoose, A., Finkel'stein, A.M.: *Science* **310**, 289 (2005)
3. Denteneer, P.J.H., Scalettar, R.T., Trivedi, N.: *Phys. Rev. Lett.* **83**, 4610 (1999)
4. Chiesa, S., Chakraborty, P.B., Pickett, W.E., Scalettar, R.T.: *Phys. Rev. Lett.* **101**, 086401 (2008)
5. Georges, A., Kotliar, G., Krauth, W., Rozenberg, M.J.: *Rev. Mod. Phys.* **68**, 13 (1996)
6. Tanasković, D., Dobrosavljević, V., Abrahams, E., Kotliar, G.: *Phys. Rev. Lett.* **91**, 066603 (2003)
7. Dobrosavljević, V., Kotliar, G.: *Phys. Rev. Lett.* **78**, 3943 (1997)
8. Miranda, E., Dobrosavljević, V.: *Rep. Prog. Phys.* **68**, 2337 (2005)
9. Andrade, E.C., Miranda, E., Dobrosavljević, V.: *Physica B* **404**, 3167 (2009)
10. Miranda, E., Dobrosavljević, V.: *Phys. Rev. Lett.* **86**, 264 (2001)
11. Andrade, E.C., Miranda, E., Dobrosavljević, V.: *Phys. Rev. Lett.* **102**, 206403 (2009)
12. Andrade, E.C., Miranda, E., Dobrosavljević, V.: *Phys. Rev. Lett.* **104**, 236401 (2010)
13. Herbut, I.F.: *Phys. Rev. B* **63**, 113102 (2001)
14. Heidarian, D., Trivedi, N.: *Phys. Rev. Lett.* **93**, 126401 (2004)
15. Mahan, G.D.: *Many-Particle Physics*, 3rd edn. Plenum, New York (2000)
16. Kotliar, G., Ruckenstein, A.E.: *Phys. Rev. Lett.* **57**, 1362 (1986)
17. Brinkman, W.F., Rice, T.M.: *Phys. Rev. B* **2**, 4302 (1970)
18. Simion, G.E., Giuliani, G.F.: *Phys. Rev. B* **72**, 045127 (2005)
19. Müller-Hartmann, E.: *Z. Phys. B* **76**, 211 (1989)
20. Vollhardt, D.: *Rev. Mod. Phys.* **56**, 99 (1984)
21. Hewson, A.C.: *The Kondo Problem to Heavy Fermions*, 1st edn. Cambridge University Press, Cambridge (1993)
22. Meyer, D., Hewson, A.C., Bulla, R.: *Phys. Rev. Lett.* **89**, 196401 (2002)
23. Vojta, M.: *Adv. Phys.* **58**, 699 (2009)
24. Littlewood, P.: *Nat. Mater.* **10**, 726 (2011)
25. Poccia, N., et al.: *Nat. Mater.* **10**, 733 (2011)
26. Dobrosavljević, V.: In: Abrahams, E. (ed.) *50 Years of Anderson Localization*. World Scientific, Singapore (2010). [arXiv: 1003.3215v1](https://arxiv.org/abs/1003.3215v1)